P H Y S I C A L   R E V I E W   L E T T E R S

From Electromagnetically Induced Transparency to Superscattering with a Single Structure: A Coupled-Mode Theory for Doubly Resonant Structures

Lieven Verslegers,* Zongfu Yu, Zhichao Ruan, Peter B. Catrysse, and Shanhui Fan[†]

E. L. Ginzton Laboratory and Department of Electrical Engineering, Stanford University, Stanford, California 94305, USA
(Received 2 October 2011; published 22 February 2012)

We observe from simulations that a doubly resonant structure can exhibit spectral behavior analogous to electromagnetically induced transparency, as well as superscattering, depending on the excitation. We develop a coupled-mode theory that explains this behavior in terms of the orthogonality of the radiation patterns of the eigenmodes. These results provide insight in the general electromagnetic properties of photonic nanostructures and metamaterials.

The concept of a cross section is very commonly used to describe how large an object appears to incident external radiation [1]. The deviation of the electromagnetic cross section with respect to the geometrical cross section is well documented for nanoscale objects. In cloaking, for example, the electromagnetic cross section is made much smaller than the geometrical cross section of the object [2–4]. For subwavelength objects exhibiting a single resonance, on the other hand, the electromagnetic cross section can be much larger than the geometrical cross section [5]. Such a resonance effect is important for applications such as in the design of electrically small antennas to allow for good transmission or reception. An important question to pose further would be: How does the electromagnetic cross section behave for an object that supports multiple resonances?

The question we pose above is, in fact, of essential importance in understanding a wide variety of effects that are of current interest in nanophotonics [6–10]. For example, it is known that having two resonances may lead to interference, in which case the spectral behavior is an optical analogue of electromagnetically induced transparency (EIT) [11–18]. For isolated objects then, this may result in a suppression of the electromagnetic cross section. On the other hand, the effect of superscattering, which also uses at least two resonances, was also recently noted. In this case, the scattering cross section is significantly enhanced due to the simultaneous presence of both resonances [19,20]. A formalism that elucidates the occurrence of both behaviors has never been proposed before.

In this Letter, as a model system of an isolated object that exhibits two resonances, we study a system consisting of two slits in a metal film and study the transmission cross section of this system for light incident on one side of the film. The transmission cross section is defined as the total transmitted power over the intensity of an incident plane wave. It is known that each slit can support a localized resonance, and hence the transmission cross section of the individual slit has a well-known Lorentzian line shape

[21,22]. The two-slit system therefore supports two resonances. For this system, our simulations reveal that it can exhibit both EIT and superscattering behavior, depending on the excitation. We develop a coupled-mode theory that explains this effect. The theory identifies a superradiant and a subradiant mode in this system [7–9,14] and, moreover, indicates the importance of the degree of orthogonality of the radiation patterns of the subradiant and superradiant eigenmodes in explaining the transmission behavior. In particular, we demonstrate that the perfect EIT analogue shows up as an extreme case where the radiation patterns of the eigenmodes are identical, up to a constant phase factor. Enhancement of the transmission cross section (i.e., superscattering), on the other hand, becomes more likely when the radiation patterns are less correlated and, moreover, is guaranteed when the radiation patterns of the eigenmodes are orthogonal and when one uses an excitation that significantly excites both resonances.

As a starting point, we simulate the transmission cross section spectrum $\sigma_T(\omega)$, of a double-slit structure in a perfect electric conductor film of thickness t [Fig. 1]. The slit widths are deep-subwavelength ($t/10 \ll \lambda$), so that the individual slits are, to a good approximation, isotropic radiators [22]. The slits are spaced $0.6t$ (center to center) and are filled with materials with a slightly different permittivity (40 and 40.16), which allows us to independently tune the resonant frequencies of the slits. We obtain $\sigma_T(\omega)$ from finite-difference frequency-domain simulations [23] [red dots in Fig. 1], for an incoming transverse magnetic plane wave (magnetic field vector pointing out of the plane). The spectral behavior is characterized by two resonances: a broad one and a narrow one. It also strongly depends on the excitation: For normal incidence and 20° off-normal incidence, the narrow resonance interferes destructively with the broad resonance, and $\sigma_T(\omega)$ exhibits an EIT line shape [Figs. 1(a) and 1(b)]; for 40° and 60° off-normal incidence, the contributions from the resonances add up and a peak is observed (superscattering) [Figs. 1(c) and 1(d)]. The position of the sharp resonance
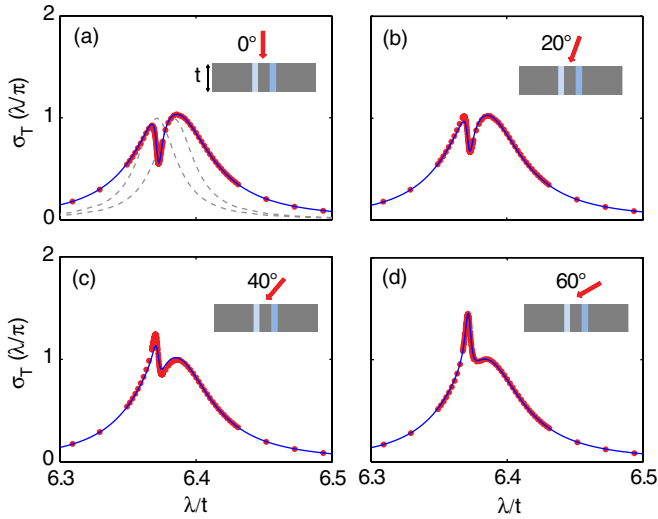
FIG. 1 (color online). Doubly resonant structures can exhibit behavior that is (a),(b) a classical analogue of EIT, as well as (c),(d) akin to superscattering in their transmission cross section spectra, depending on the excitation. Theory (blue line) matches finite-difference frequency-domain simulations (red dots). The insets show the simulated double-slit structure with broken symmetry (permittivities of materials in the slits are 40 and 40.16) and the incident plane wave. The dashed lines correspond to the Lorentzian transmission cross section spectra of the individual slits.

with respect to the narrow resonance remains approximately unchanged as the angle of incidence is varied.

In order to explain this behavior, we develop a coupled-mode theory. In this coupled-mode theory, the slits are described as resonances, with amplitudes $\mathbf{a} = [a_1\ a_2]^T$. These resonances interact with free space on both sides of the film. The free space is characterized in terms of plane wave channels, for which the amplitudes of incoming and outgoing waves are denoted s_+ and s_-, respectively. We distinguish between plane wave channels that are above (subscript T) or below (subscript B) the film. To facilitate the description of these plane wave channels, we impose a periodic boundary condition with period L and label the channels with respect to the parallel wave vector components of $2\pi n/L$, with n being integers [22,24]. For propagating modes, the index n takes on integer values from $-N$ to N, with $N = \lfloor \frac{L}{\lambda} \rfloor$, where λ is the wavelength. An index n corresponds to a channel with angle $\theta_n = \arcsin(\frac{n}{N})$ with the normal. In the end of the calculation, we will take the limit $L \to \infty$ to recover the case of an isolated object interacting with a continuum of plane wave channels. Once the resonances and channels are defined, the coupled-mode equations can be written as [25–27]

$$\frac{d\mathbf{a}}{dt} = (i\Omega - \Gamma)\mathbf{a} + K^T s_{T,+}, \qquad s_{B,-} = K\mathbf{a}. \quad (1)$$

The matrix

$$\Omega = \begin{bmatrix} \omega_1 & \omega_{12} \\ \omega_{12} & \omega_2 \end{bmatrix}$$

contains the resonant frequencies ω_1 and ω_2 and the direct coupling term ω_{12};

$$\Gamma = K^+ K = \begin{bmatrix} \gamma_1 & \sqrt{\gamma_1\gamma_2}x \\ \sqrt{\gamma_1\gamma_2}x & \gamma_2 \end{bmatrix}$$

contains the amplitude leakage rates γ_1 and γ_2 of the resonators. The form of these equations is dictated by energy conservation and time-reversal symmetry [26]. The off-diagonal elements of Γ describe the indirect coupling between the resonances, as induced by the interaction between each resonance and free space. These elements depend on x, defined as

$$x = \lim_{N\to\infty} \frac{1}{N\pi} \sum_{n=-N}^{N} \frac{e^{i\phi_n}}{\cos\theta_n} = \frac{1}{\pi}\int_{-\pi/2}^{\pi/2} e^{i\phi}d\theta = J_0\left(\frac{2\pi}{\lambda}d\right),$$

$$(2)$$

with $\phi_{(n)} = \frac{2\pi}{\lambda}d\sin\theta_{(n)}$ [Fig. 2(a)]. x characterizes the overlap between the radiation patterns of the *individual* resonators, here assumed isotropic. For $d = 0$, $x = 1$, describing the hypothetical case where the two slits are right on top of each other, and hence their radiation patterns are identical. As d increases, x oscillates towards zero, following a zeroth order Bessel function of the first kind J_0 [Fig. 2(b)].

The coupling constants to the individual channels, in matrix form, are

$$K^T = \begin{bmatrix} k_{-N,1} & \cdots & k_{0,1} & \cdots & k_{N,1} \\ k_{-N,2} & \cdots & k_{0,2} & \cdots & k_{N,2} \end{bmatrix}$$

$$= \frac{1}{\sqrt{N\pi}}$$

$$\times \begin{bmatrix} \sqrt{\frac{\gamma_1}{\cos\theta_{-N}}} & \cdots & \sqrt{\gamma_1} & \cdots & \sqrt{\frac{\gamma_1}{\cos\theta_N}} \\ \sqrt{\frac{\gamma_2}{\cos\theta_{-N}}}e^{i\phi_{-N}} & \cdots & \sqrt{\gamma_2} & \cdots & \sqrt{\frac{\gamma_2}{\cos\theta_N}}e^{i\phi_N} \end{bmatrix}.$$
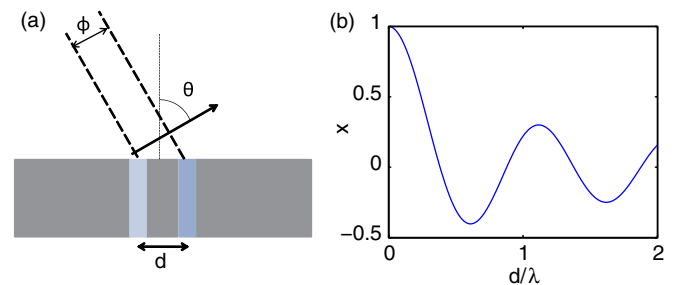
$$(3)$$

FIG. 2 (color online). (a) Two deep-subwavelength slits spaced a distance d couple to an outgoing plane wave (under an angle θ with the normal) with phase difference ϕ. The slits are assumed to be isotropic radiators. (b) Overlap between the radiation patterns of the individual radiators.

Assuming a plane wave excitation in the top half space, under normal incidence,

$$s_{T,+} = [\,0\quad\ldots\quad 0\quad 1\quad 0\quad\ldots\quad 0\,]^T. \qquad (4)$$

Similarly, for a plane wave under an angle θ_n, all channels have zero amplitude, except for channel n. The amplitudes of the channels in the bottom half space are given by the vector $s_{B,-}$. The transmission cross section is then defined as

$$\sigma_T(\omega,\theta_n) = \frac{s_{B,-}^+ - s_{B,-}}{|s_{T,n+}|^2/(L\cos\theta_n)}, \qquad (5)$$

with

$$s_{B,-} = K[i(\omega I - \Omega) + \Gamma]^{-1} K^T s_{T,+}, \qquad (6)$$

which leads to [28]

$$
\begin{aligned}
\sigma_T(\omega,\theta_n) = \frac{2\lambda}{\pi}\Big[&-\omega_{12}(\cos\phi_n + x)(\sqrt{\gamma_1}\gamma_2^{3/2}\omega_1 + \gamma_1^{3/2}\sqrt{\gamma_2}\omega_2 - \gamma_1^{3/2}\sqrt{\gamma_2}\omega - \sqrt{\gamma_1}\gamma_2^{3/2}\omega) \\
&+ (x\cos\phi_n - 1)(\gamma_1^2\gamma_2^2 - \gamma_1^2\gamma_2^2 x^2) - \gamma_1\gamma_2 x\cos\phi_n(\omega_{12}^2 + \omega^2 + \omega_1\omega_2 - \omega\omega_2 - \omega\omega_1) - \gamma_1\gamma_2\omega_{12}^2 \\
&+ \gamma_1^2\omega\omega_2 + \gamma_2^2\omega\omega_1 - \frac{\gamma_2^2(\omega_1^2 + \omega^2) + \gamma_1^2(\omega_2^2 + \omega^2)}{2}\Big] \Big/ \{[2\sqrt{\gamma_1\gamma_2}x\omega_{12} + (\gamma_1 + \gamma_2)\omega - \gamma_2\omega_1 - \gamma_1\omega_2]^2 \\
&+ (-\gamma_1\gamma_2 x^2 + \gamma_1\gamma_2 + \omega_{12}^2 - \omega^2 + \omega\omega_1 + \omega\omega_2 - \omega_1\omega_2)^2\}.
\end{aligned}
\qquad (7)
$$

This equation matches the simulations excellently [blue lines in Fig. 1]. The resonant frequency ω_1 and ω_2 and (amplitude) leakage rates γ_1 and γ_2 were found from first-principles electromagnetic simulations of the single slits [dashed lines in Fig. 1(a)]. We note that the broad (narrow) resonance is wider (sharper) than either one of the individual resonances, indicating that the superradiant and subradiant eigenresonances of the system resulted from the coupling of the individual resonances. The direct coupling term ω_{12} is easily fitted, since it corresponds to about half the difference in position of the broad and narrow peaks. We can therefore use a single simulation to extract this parameter, which in turn allows us to analytically calculate the spectral response for any angle of incidence. Alternatively, this coupling constant can be calculated analytically in principle [25]. In the structure simulated here, the direct coupling term is small, and the broad and narrow resonances are closely aligned. For stronger direct coupling, the resonances become less aligned and the line shape becomes more Fano-like.

To gain more insight, we now develop an approximate theory that identifies the subradiant and superradiant eigenmodes. For this theory, we can assume that $\gamma_1 = \gamma_2 = \gamma$, because similar slits have approximately the same leakage rates. Furthermore, we assume that the spatial separation is small compared to the wavelength. In that case, x does not strongly depend on the choice of wavelength λ, so that we can pick $x = x(\lambda_0)$ for a wavelength λ_0 in the range of interest.

Under these assumptions, we can find the eigenmodes, labeled a and b, of the matrix $j\Omega - \Gamma$:

$$v_{a,b} \sim \left[\frac{-\omega_{12}i + \gamma x}{\frac{\omega_1-\omega_2}{2}i \pm \frac{1}{2}\sqrt{-(\omega_1-\omega_2)^2 + (2\omega_{12}i - 2\gamma x)^2}}\quad 1\right] \qquad (8)$$

as well as the corresponding eigenvalues $i\omega_{a,b} - \gamma_{a,b}$, where

$$
\begin{aligned}
\gamma_{a,b} = -\mathrm{Re}\Big[&\frac{\omega_1 + \omega_2}{2}i - \gamma \mp \frac{1}{2} \\
&\times \sqrt{-(\omega_1-\omega_2)^2 + (2\omega_{12}i - 2\gamma x)^2}\Big],
\end{aligned}
$$

$$
\begin{aligned}
\omega_{a,b} = \mathrm{Im}\Big[&\frac{\omega_1 + \omega_2}{2}i - \gamma \mp \frac{1}{2} \\
&\times \sqrt{-(\omega_1-\omega_2)^2 + (2\omega_{12}i - 2\gamma x)^2}\Big].
\end{aligned}
\qquad (9)
$$

These eigenmodes have the same resonant frequency, when $\omega_{12} = 0$. Eigenmode a is superradiant; eigenmode b is subradiant. The (complex) radiation patterns of the eigenmodes are calculated by using the elements of the eigenvectors v_a and v_b:

$$
\begin{aligned}
C_a(\theta) &= v_{a,1} + v_{a,2}e^{i\phi}, \\
C_b(\theta) &= v_{b,1} + v_{b,2}e^{i\phi}.
\end{aligned}
\qquad (10)
$$

These radiation patterns satisfy the normalization relation $\frac{1}{\pi}\int_{-\pi/2}^{\pi/2} C_a^*(\theta)C_a(\theta)d\theta = \frac{1}{\pi}\int_{-\pi/2}^{\pi/2} C_b^*(\theta)C_b(\theta)d\theta = 1$. $|C_a(\theta)|^2$ and $|C_b(\theta)|^2$ are therefore directivities of the radiation patterns of the eigenmodes.

We define the radiation overlap:

$$h = \frac{1}{\pi}\int_{-\pi/2}^{\pi/2} C_b'^*(\theta)C_a'(\theta)d\theta. \qquad (11)$$

with

$$C_a'(\theta) = v_{a,1} - v_{a,2}e^{i\phi}, \quad C_b'(\theta) = v_{b,1} - v_{b,2}e^{i\phi}. \qquad (12)$$

The phase of h corresponds to a weighed radiation phase difference between the superradiant and subradiant eigenmodes. With these definitions, for a plane wave coming in

under an angle θ_{exc}, the transmission cross section can be written in a much more compact form as

$$\sigma_T(\omega, \theta_{\mathrm{exc}}) \approx \frac{p\lambda}{\pi}\left\{ \frac{|C_a(\theta_{\mathrm{exc}})|^2\gamma_a^2}{(\omega - \omega_a)^2 + \gamma_a^2} + \frac{|C_b(\theta_{\mathrm{exc}})|^2\gamma_b^2}{(\omega - \omega_b)^2 + \gamma_b^2} \right.$$
$$\left. - 2\,\mathrm{Re}\left[\frac{C_a^*(\theta_{\mathrm{exc}})C_b(\theta_{\mathrm{exc}})h\gamma_a\gamma_b}{(-i(\omega - \omega_a) + \gamma_a)(i(\omega - \omega_b) + \gamma_b)} \right] \right\}$$

$$(13)$$

with prefactor $p = \frac{\gamma^2}{\gamma_a\gamma_b|v_{a,1}v_{b,2} - v_{b,1}v_{a,2}|^2}$. Under the stated assumptions, the result of the approximate theory [Eq. (13)] is in close agreement with Eq. (7) [28].

In Eq. (13), the two Lorentzians describe the contributions of the individual eigenmodes, and the cross term describes their interference. At $\omega = \omega_a = \omega_b$ (assuming $\omega_{12} = 0$), the spectrum will show a dip (EIT) when $\gamma_a \gg \gamma_b$ and

$$|C_a(\theta_{\mathrm{exc}})|^2 + |C_b(\theta_{\mathrm{exc}})|^2 - 2\,\mathrm{Re}[C_a^*(\theta_{\mathrm{exc}})C_b(\theta_{\mathrm{exc}})h]$$
$$< |C_a(\theta_{\mathrm{exc}})|^2$$
$$\Leftrightarrow |C_b(\theta_{\mathrm{exc}})|^2 - 2\,\mathrm{Re}[C_a^*(\theta_{\mathrm{exc}})C_b(\theta_{\mathrm{exc}})h] < 0, \quad (14)$$

and a peak (superscattering) when

$$|C_b(\theta_{\mathrm{exc}})|^2 - 2\,\mathrm{Re}[C_a^*(\theta_{\mathrm{exc}})C_b(\theta_{\mathrm{exc}})h] > 0. \quad (15)$$

From Eq. (14), we see that EIT is more likely for larger overlap between the radiation patterns of the eigenmodes, i.e., values of $|h|$ close to 1. Strong interference between the two resonant pathways can be accomplished only when the radiation patterns of the subradiant and superradiant modes are similar to each other. We also note the importance of the phase difference between the eigenmodes upon excitation [the phase of $C_a^*(\theta_{\mathrm{exc}})C_b(\theta_{\mathrm{exc}})$] and the weighed phase difference in radiation (the phase of h). To achieve a prominent EIT behavior, one has to achieve destructive interference; thus, these phases need to cancel each other out. Perfect EIT occurs when the radiation patterns of the eigenmodes are identical, up to a constant phase factor: $C_a(\theta) \sim C_b(\theta)$ and $|h| = 1$. The transmission cross section is then

$$\sigma_T(\omega, \theta_{\mathrm{exc}}) \approx \frac{p\lambda}{\pi}|C_a(\theta_{\mathrm{exc}})|^2 \left| \frac{\gamma_a}{i(\omega - \omega_a) + \gamma_a} \right.$$
$$\left. - \frac{\gamma_b}{i(\omega - \omega_b) + \gamma_b} \right|^2, \quad (16)$$

so that the transmission cross section drops to exactly zero at $\omega = \omega_a = \omega_b$. Figure 3(a) illustrates this case, with the following parameters: $\omega_a = \omega_b = 1$, $\gamma_a = 0.39$, $\gamma_b = 0.01$, $|C_a(\theta)| = |C_b(\theta)| = 1$, and $p = 1$.

Another extreme, the case of omnidirectional superscattering, can be achieved in structures such as nanorods and nanospheres with a plasmonic-dielectric-plasmonic layer structure [19,20], where the radiation patterns of the subradiant and superradiant eigenmodes are exactly
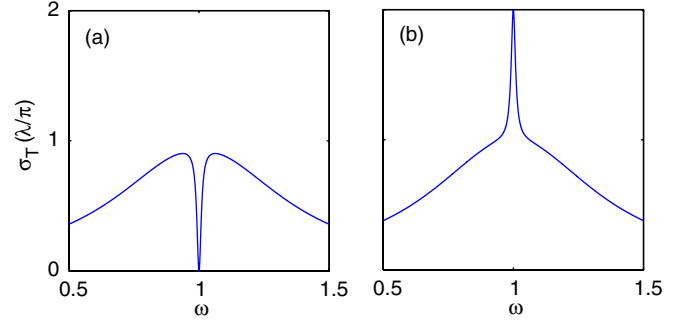

FIG. 3 (color online).   Transmission cross section spectra for (a) perfect omnidirectional EIT and (b) omnidirectional superscattering.

orthogonal, so that $h = 0$. Equation (15) is then guaranteed to be satisfied, when the subradiant eigenmode is excited. The transmission cross section is then nothing more than the sum of the Lorentzians associated with the individual eigenmodes. For a structure that supports two such eigenmodes, we find

$$\sigma_T(\omega, \theta_{\mathrm{exc}}) \approx \frac{p\lambda}{\pi}\left[\frac{|C_a(\theta_{\mathrm{exc}})|^2\gamma_a^2}{(\omega - \omega_a)^2 + \gamma_a^2} + \frac{|C_b(\theta_{\mathrm{exc}})|^2\gamma_b^2}{(\omega - \omega_b)^2 + \gamma_b^2} \right].$$
$$(17)$$

This case is illustrated in Fig. 3(b), with the same parameters as before, except that now $h = 0$. Note that under the assumption that $|C_a(\theta)| = |C_b(\theta)| = 1$, the radiation patterns can still be orthogonal leading to $h = 0$, given that the (complex) radiation patterns have the right phase relation.

The two-slit case that we have considered in Fig. 1 corresponds to the intermediate case, where there is a partial overlap between the radiation patterns of the eigenmodes. For the two slits in Fig. 1, $|h|$ is about 0.7, significantly smaller than 1 and larger than 0. In such a case, depending on θ_{exc}, either Eq. (14) or Eq. (15) can be satisfied, so that we can switch from EIT to superscattering. For normal incidence and 20° off-normal incidence, Eq. (14) is satisfied. We observe weakened EIT behavior: The transmission cross section shows a dip, but not to zero, because the radiation patterns cannot perfectly destructively interfere, for only partial radiation overlap [Figs. 1(a) and 1(b)]. Superscattering behavior, i.e., the existence of a subradiant peak on top of a superradiant background, occurs for the two-slit case for sufficiently large off-normal angles of incidence [Figs. 1(c) and 1(d)]. The subradiant and superradiant eigenmodes are then excited with an amplitude and phase relation that causes Eq. (15) to be satisfied. We have thus provided a theory that accounts for the simultaneous presence of EIT and superscattering for the structure shown in Fig. 1.

In conclusion, we developed a coupled-mode theory that predicts and explains EIT analogues in addition to superscattering in doubly resonant structures in terms of the

overlap between the radiation pattern of subradiant and superradiant eigenmodes. This theory provides insights in the general spectral behavior for metamaterials, as well as optical antennas [29,30] and nanoparticles [31,32].

*Corresponding authors.
lieven.verslegers@gmail.com
†shanhui@stanford.edu

[1] C. F. Bohren and D. R. Huffman, *Absorption and Scattering of Light by Small Particles* (Wiley, New York, 1983).

[2] D. Schurig, J. J. Mock, B. J. Justice, S. A. Cummer, J. B. Pendry, A. F. Starr, and D. R. Smith, Science **314**, 977 (2006).

[3] U. Leonhardt, Science **312**, 1777 (2006).

[4] A. Alu and N. Engheta, Phys. Rev. Lett. **100**, 113901 (2008).

[5] M. Husnik, M. W. Klein, N. Feth, M. König, J. Niegemann, K. Busch, S. Linden, and M. Wegener, Nature Photon. **2**, 614 (2008).

[6] B. Luk'yanchuk, N. I. Zheludev, S. A. Maier, N. J. Halas, P. Nordlander, H. Giessen, and C. T. Chong, Nature Mater. **9**, 707 (2010).

[7] A. E. Miroshnickenko, S. Flach, and Y. S. Kivshar, Rev. Mod. Phys. **82**, 2257 (2010).

[8] J. A. Fan, C. Wu, K. Bao, J. Bao, R. Bardhan, N. J. Halas, V. N. Manoharan, P. Nordlander, G. Shvets, and F. Capasso, Science **328**, 1135 (2010).

[9] Z. Ruan and S. Fan, J. Phys. Chem. C **114**, 7324 (2010).

[10] N. Liu, A. P. Alivisatos, M. Hentschel, T. Weiss, and H. Giessen, Science **332**, 1407 (2011).

[11] K. J. Boller, A. Imamoglu, and S. E. Harris, Phys. Rev. Lett. **66**, 2593 (1991).

[12] N. Papasimakis, V. A. Fedotov, N. I. Zheludev, and S. L. Prosvirnin, Phys. Rev. Lett. **101**, 253903 (2008).

[13] N. Liu, L. Langguth, T. Weiss, J. Kästel, M. Fleischhauer, T. Pfau, and H. Giessen, Nature Mater. **8**, 758 (2009).

[14] S. Zhang, D. A. Genov, Y. Wang, M. Liu, and X. Zhang, Phys. Rev. Lett. **101**, 047401 (2008).

[15] P. Tassin, L. Zhang, T. Koschny, E. N. Economou, and C. M. Soukoulis, Phys. Rev. Lett. **102**, 053901 (2009).

[16] V. A. Fedotov, M. Rose, S. L. Prosvirnin, N. Papasimakis, and N. I. Zheludev, Phys. Rev. Lett. **99**, 147401 (2007).

[17] S.-Y. Chiam, R. Singh, C. Rockstuhl, F. Lederer, W. Zhang, and A. A. Bettiol, Phys. Rev. B **80**, 153103 (2009).

[18] A. Artar, A. A. Yanik, and H. Altug, Nano Lett. **11**, 1685 (2011).

[19] Z. Ruan and S. Fan, Phys. Rev. Lett. **105**, 013901 (2010).

[20] Z. Ruan and S. Fan, Appl. Phys. Lett. **98**, 043101 (2011).

[21] Y. Takakura, Phys. Rev. Lett. **86**, 5601 (2001).

[22] L. Verslegers, Z. Yu, P. B. Catrysse, Z. Ruan, and S. Fan, J. Opt. Soc. Am. B **27**, 1947 (2010).

[23] G. Veronis and S. Fan, in *Surface Plasmon Nanophotonics*, edited by M. L. Brongersma and P. G. Kik (Springer, New York, 2007), p. 169.

[24] Z. Yu, A. Raman, and S. Fan, Proc. Natl. Acad. Sci. U.S.A. **107**, 17491 (2010).

[25] H. A. Haus, *Waves and Fields in Optoelectronics* (Prentice-Hall, Englewood Cliffs, NJ, 1984).

[26] W. Suh, Z. Wang, and S. Fan, IEEE J. Quantum Electron. **40**, 1511 (2004).

[27] R. E. Hamam, A. Karalis, J. D. Joannopoulos, and M. Soljacic, Phys. Rev. A **75**, 053801 (2007).

[28] See Supplemental Material at http://link.aps.org/supplemental/10.1103/PhysRevLett.108.083902 for a detailed derivation.

[29] P. Bharadwaj, B. Deutsch, and L. Novotny, Adv. Opt. Photon. **1**, 438 (2009).

[30] L. Cao, P. Fan, and M. L. Brongersma, Nano Lett. **11**, 1463 (2011).

[31] Y. Sonnefraud, N. Verellen, H. Sobhani, G. A. E. Vandenbosch, V. V. Moshchalkov, P. Van Dorpe, P. Nordlander, and S. A. Maier, ACS Nano **4**, 1664 (2010).

[32] T. J. Davis, K. C. Vernon, and D. E. Gómez, Phys. Rev. B **79**, 155423 (2009).